

Structural Geophysics Investigations using GIS and DC Resistivity Techniques: Hydrogeological Implications of Wadi Ramleiya, Eastern Desert, Egypt

Mohamed A. Attwa^{1,2} and Abdelhalim M. Ali²

¹Structural Geophysics Group (SGG), Geology Department, Faculty of Science
Zagazig University, Egypt

²Geology department, The National Authority for Remote Sensing and Space Sciences (NARSS)
Egypt

*Corresponding author's email: attwa_m2 [AT] yahoo.com

ABSTRACT-- *In this study, an integrated suite of geological and direct current resistivity (DCR) data is used to evaluate the hydrogeophysical conditions at the downstream part of Wadi Ramleiya, Eastern Desert, Egypt. Remote-sensing (RS) and geographic information system (GIS) techniques are used to demonstrate the geological and morphometric characteristics of drainage basins. DCR measurements in the form of 1D and 2D surveys are carried out to reveal the subsurface layer distributions and demonstrate the groundwater potentialities. It is obviously that the shallow aquifers and groundwater flow direction are related to structural controls. Based on the inversion results of DCR data, the aquifer is under unconfined conditions where it rests on layers of argillaceous limestone and overlain by gravelly sand. Accordingly, the obtained results can serve as a basis for monitoring, planning and management of water resources in such desert area, and as a whole, they constitute an encouraging example using an integrated approach of geological, morphometric and DCR data in groundwater exploration and flash-flood hazard management.*

Keywords-- GIS, DC resistivity, hydrogeological basin, morphometric analysis, Wadi Ramleiya, Egypt

1. INTRODUCTION

In Egypt, establishing expanding the existing and new urban areas becomes one of the important priorities for the decision makers. Such strategy is essentially to reduce the dense population around the Nile valley. Wadi Ramleiya area is located at the south eastern part of New Atfih city, Eastern Desert, Egypt (Figure 1). Systematic managing and planning for groundwater investigation using high and modern techniques are carried out for the proper management, utilization and protection of this critical resource.

Recently, structural geophysical methods as direct current resistivity (DCR) technique can deduce the subsurface geology and structure information with high resolution on various spatial scales [1]. Further, the 2D DCR survey has been widely used with success to image the subsurface geological structures [2, 3] to represent the sites prone to hazards [4] and to predict the hydrogeophysical parameters at the field-scale [5, 6]. Although 2D DCR survey is favored for representing lateral inhomogeneities, the DCR sounding surveys can be also considered as a considerable source of regional hydrogeological and geological information [e.g. 7, 8, 9].

Currently, remote-sensing (RS) and geographic information system (GIS) techniques are commonly used in many fields as geology, archaeology and earth observation without direct contact with the earth. Accordingly, such techniques are helpful and very effective globally in reaching inaccessible areas like rugged lands forests and oceans. RS applications are like to graphics software, but they enable generating geographic information from airborne sensor and satellite data. Without doubts RS provide accurate data as many papers had been denoted, [e.g., 10, 11, 12]

In this study, Enhanced Thematic Mapper Landsat (ETM+) images, geographic information system (GIS), hydrological modeling and DCR techniques were integrated to (i) delineate the active alluvial channels, subsurface structures and aquifer distributions. DCR method was applied in Wadi-Ramleiya area to evaluate hydrogeological potentialities using advanced inversion methods. Further, the interpretations of DCR data inversion were implemented for mapping the subsurface structures.

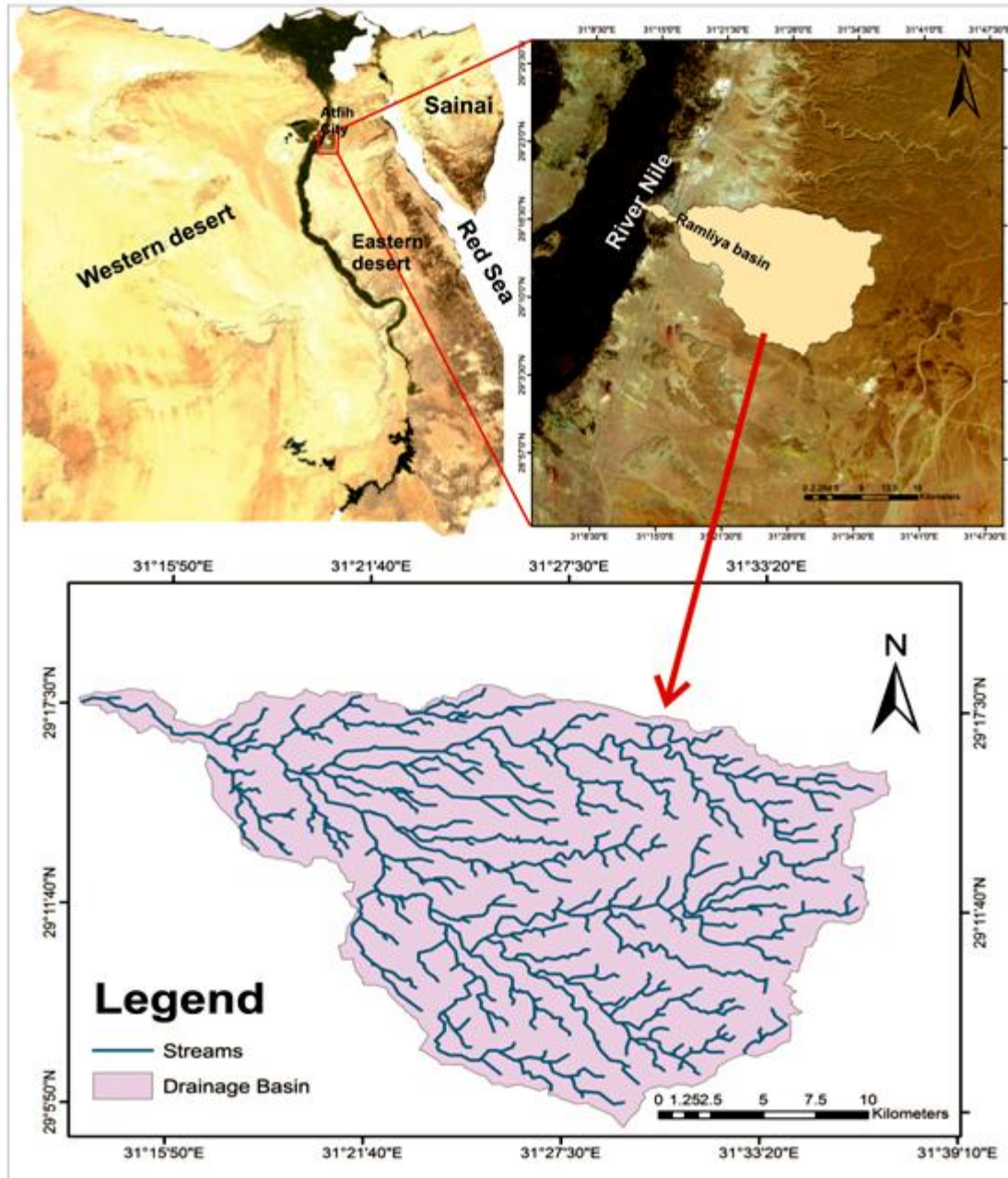


Figure (1) : Location map of Wadi-Ramleiya basin.

2. STUDY AREA AND GEOLOGICAL SETTING

Wadi Ramleiya is located in a wide extended desert area at about 6km east of the floodplain adjacent to the Nile River (Figure 1). The average of temperature goes up to 35°C in summer and comes down to 11°C in winter season. Wadi-Ramleiya area is geographically located between latitudes 29° 4' 30" , 29° 19' 30" N, and longitudes 31° 13' 30" , 31° 37' 30"E (Figure1).The desert land is dominated with Eocene rocky plateau forming the entire heights in the area. Generally, the surface exposures in this area show gradual and gentle declination in profiles towards the west until merge into the Nile flood plain.

Wadi Ramleiya are stratigraphically classified into the following rock units(Figure2): (1) Wadi Rayan Formation, Middle Eocene in age, consisting of Nummulitic limestone, haies and sandy limestone in upper part; (2) Beni-Suef Formation

of Middle Eocene age especially forming of shallow, soft marls and shale; limestone beds;(3) Observatory Formation (upper Middle Eocene in age), where the type area is Observatory Plateau, Helwan area consisting of bedded limestone, sometimes chalky; and (4) Qasr El Sagha Formation (Late Eocene in age) consisting of deltaic, intertidal, restricted lagoonal and marine facies [13].

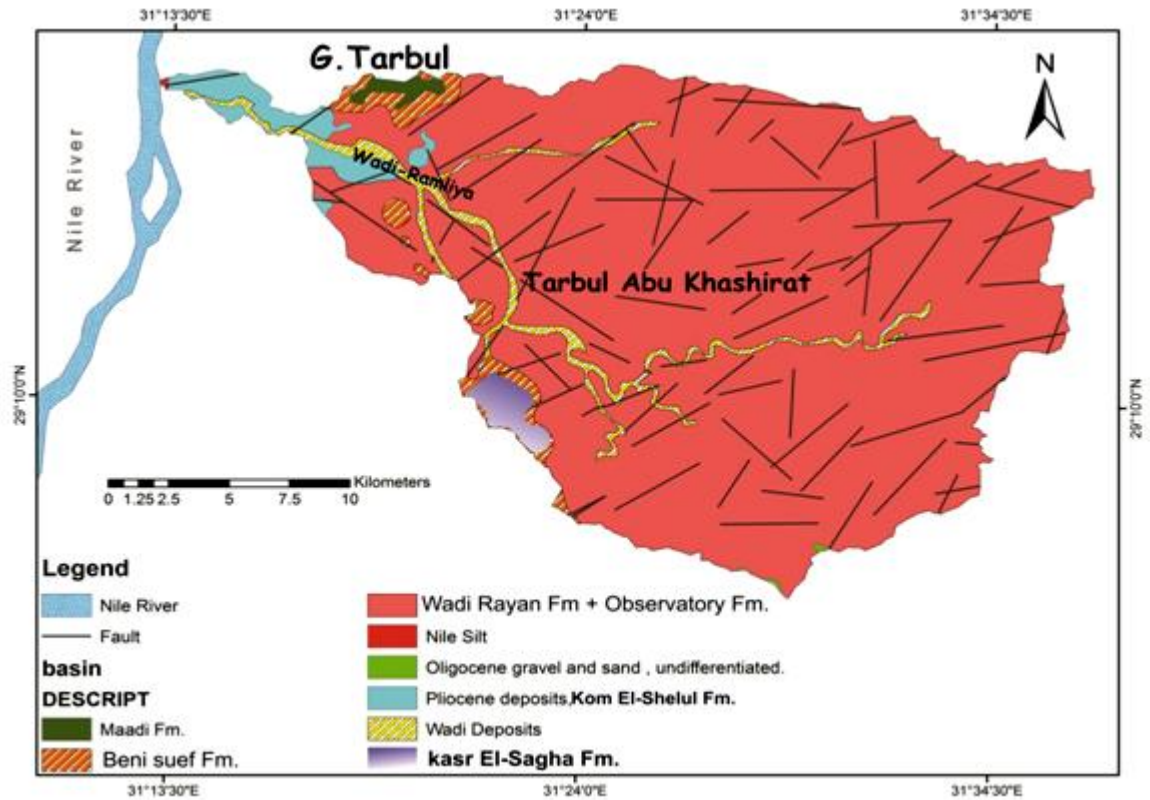


Figure (2): Geological map of Wadi-Ramleiya basin (modified after,[14]).

3. FIELD MEASUREMENTS

The electrical resistivity of a geological formation is a physical characteristic depending on the flow of electric current in the formation. Subsurface resistivity is related to several geological parameters and varies with these parameters such as texture of the rock, nature of mineralization and conductivity of electrolyte contained within the rock [15, 16].

In this study, the field surveys were achieved through gradual stages from December 2016 until August 2017. At initial DCR survey, nine DC soundings were executed (Figure3) using conventional Schlumberger array (Figure4) with 750 m maximum half electrode spacing (AB/2). Here, the DCR soundings were measured to acquire regional and deep geological information. In order to reduce the DCR ambiguity related to surface topography, the DCR soundings were measured as possible over a straight survey lines. Consequently, the DC sounding distributions were carried out based on the ground accessibility of the area, where many hills and queries are commonly found.

Figure (3) shows the distribution of resistivity soundings locations all over the area. Two sounding points were measured near to the available observation wells to conduct the resistivity spectrum and salinity prediction of the study area.

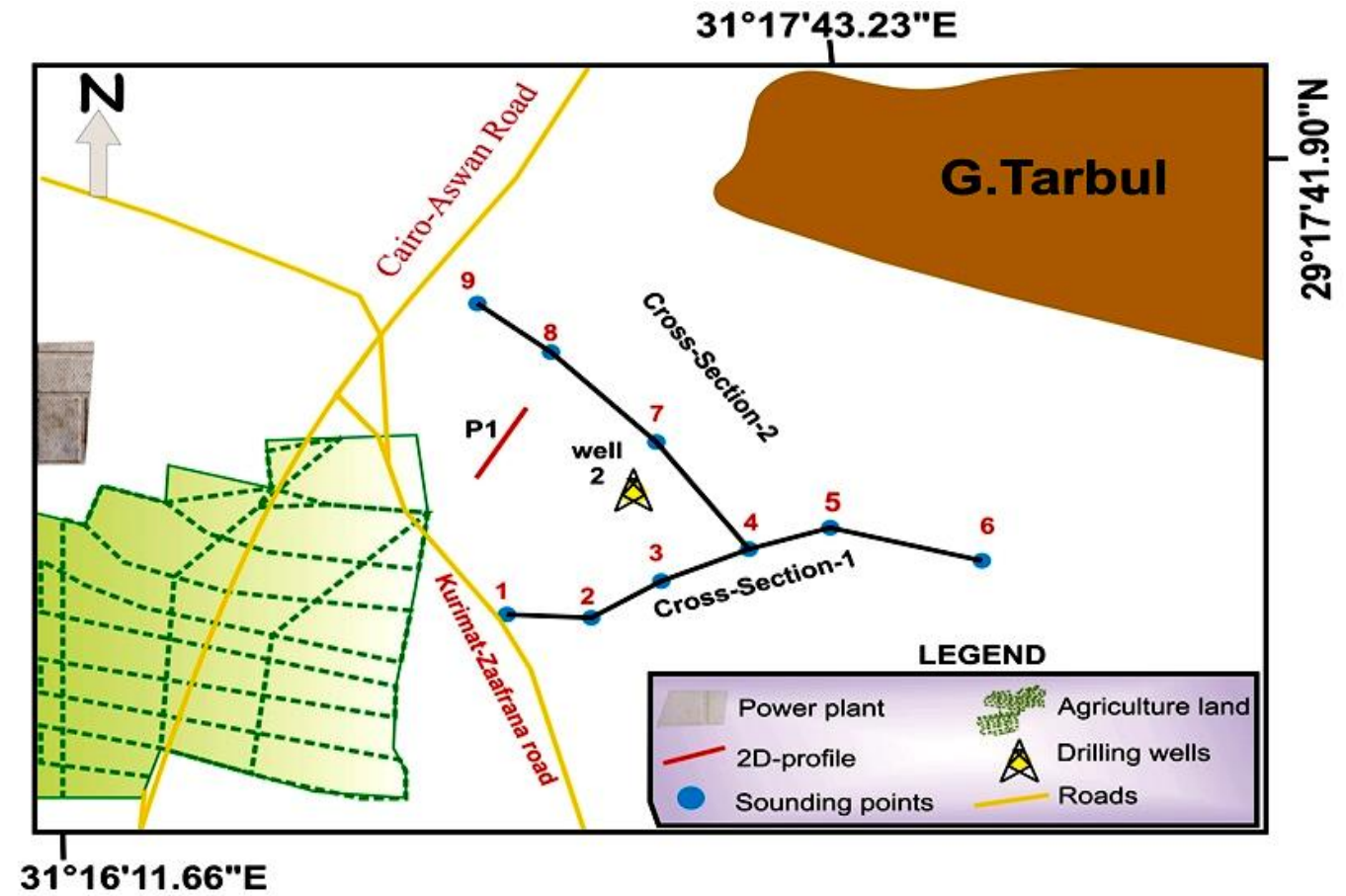


Figure (3): Location map of DCR measurements at downstream part of wadi Ramleiya, Egyptian Eastern Desert.

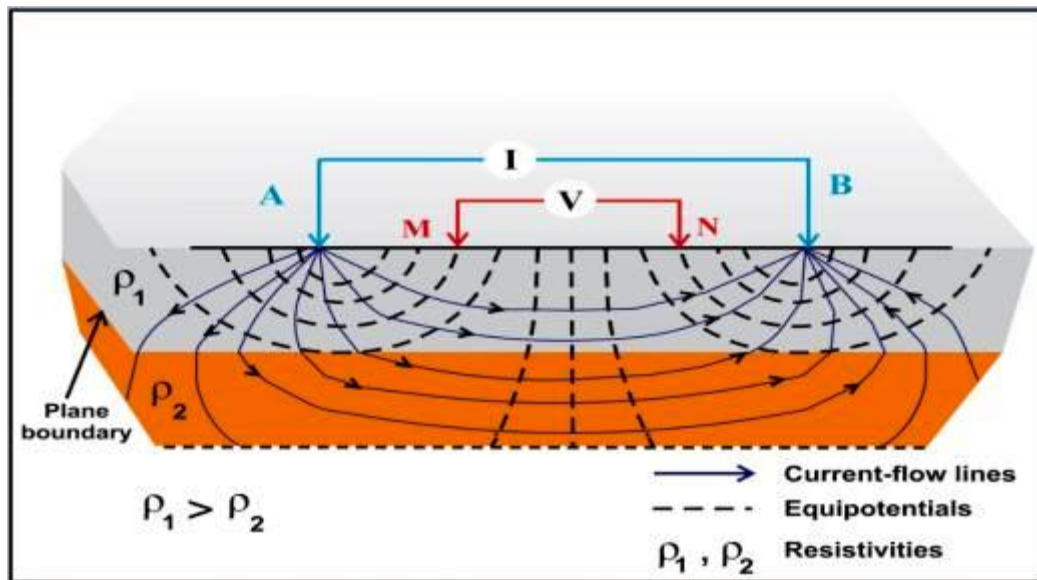


Figure (4): Principle of resistivity measurements with a four electrode configuration [17].

According to the field observations and 1D inversion results of DCR sounding points, the 2D DC resistivity surveys were conducted along one profile using Wenner beta electrode configuration (Figure5). The data acquisition began after positioning the electrodes with equal spacing along the 2D profile. Stability and precision of each measurement has been

done by making repeated readings (10-times) for each data point over a measurement. The acquired data are then used as input for the forward or inverse computer modeling programs that generate the resistivity (or electrical conductivity) depth sections. The 2D profiles (P1) were acquired on the wadi downstream to record the lateral variation of subsurface structure depending on DCR sounding results, Figure 7. The 2D P1 profile was extended perpendicular to downstream of Wadi. The length of the 2D profile was 232 m. The DCR profiling, 2D, was conducted using 30 electrodes with 8 m electrode spacing, a . This type of array is characterized by rapidly covering large areas with small spacing and good horizontal coverage [18]. As Wenner beta is a particular case of dipole-dipole (DD) array, the detection of horizontal heterogeneity within the near surface layers is expected. The total number of the measured point's 2D-ERTs was 126 for each profile. The maximum electrode spacing a , was 56 m, i.e., the maximum data level n , was 7.

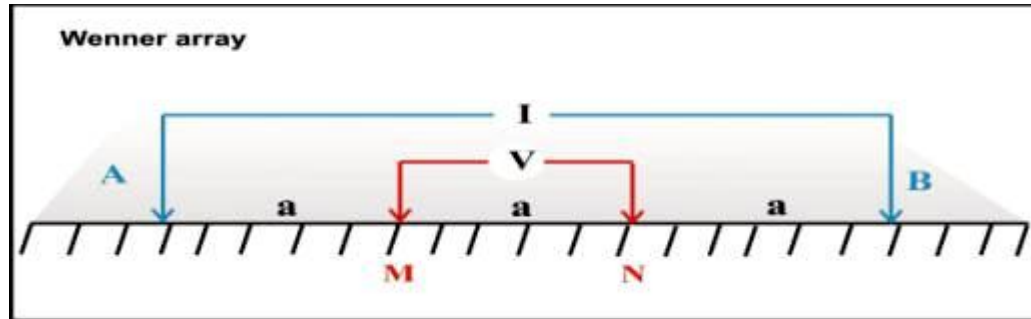


Figure (5): Wenner beta electrode configurations. The letters (A and B) denote the current electrodes, the letters (M and N) denote the potential electrodes and (a) denote the spacing between the electrodes.

4. DATA PROCESSING AND INVERSION

A first appraisal of a subsurface resistivity distribution can often be obtained by merely looking at the shapes of the field curves and the ranges of apparent resistivity values. DCR sounding data in the form of apparent resistivity and electrode spacing were interpreted qualitatively and quantitatively, in order to understand the relation between the apparent resistivity values and the parameters that define and reflect the subsurface geoelectrical layers and their extension. Consequently the prevailing hydrogeological conditions in the study areas were clarified.

In quantitative interpretation of DC sounding data (i.e., inversion process), the apparent resistivity values versus half electrode spacing ($AB/2$) are plotted to obtain the layer resistivities and thicknesses. The theoretical background is discussed in detail by [19]. Basically, the inversion process was carried out using IPI2WIN software [20] in which the measured sounding curve with calculated sounding curves were compared for given model layering. Purely automatic inversion programs without any assumptions of the layering exist as well as programs that require the handling of the interpreter. In the latter case, a starting model is defined incorporating known geological parameters (e.g., standard thicknesses of stratigraphical units, depth to the groundwater table), available borehole information and/or the results of other geophysical measurements. Regarding to the starting model, the computer conducts an iteration process by trying to adjust the theoretical model and its sounding curve to the measured curve. The inversion process is repeated until there is a good fit between the measured resistivity data and the synthetic sounding curve.

IPI2WIN software [20] is based on linear filtering as 1D forward modeling and Newton algorithm of the least number of layers to solve the inverse problem. The main advantage of this program is that the interpretation is presented along a profile where its points are treated as a unity representing the subsurface layers of the survey area as a whole. The inversion process will stop the iteration at the best fit between the starting model and the observed apparent resistivity. Some model parameters (depth of layers) were fixed during interpretation procedures according to the available geological data which were obtained from the surface exposures, drilled boreholes and geological investigations. Figure (6) shows that all the available layer thicknesses, which obtained from available wells are introduced as a ground truth.

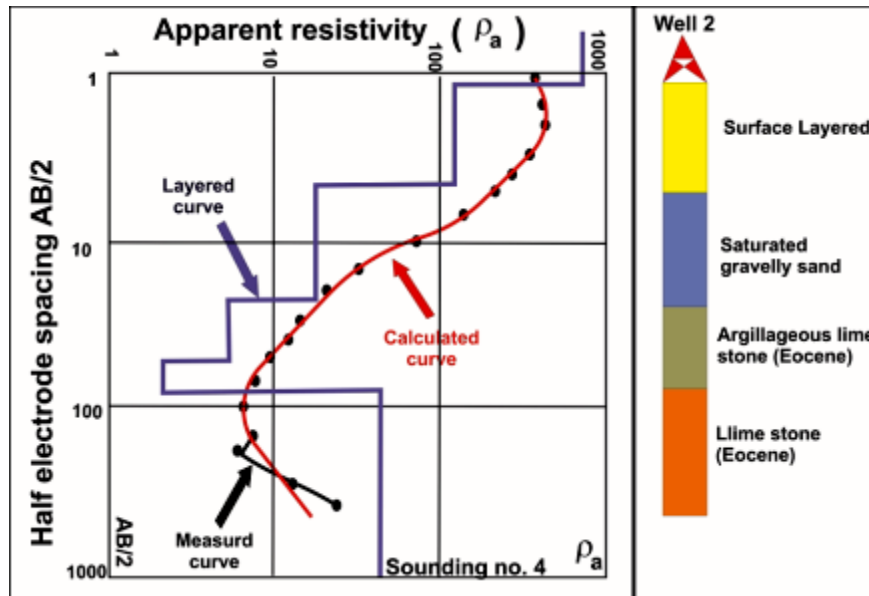
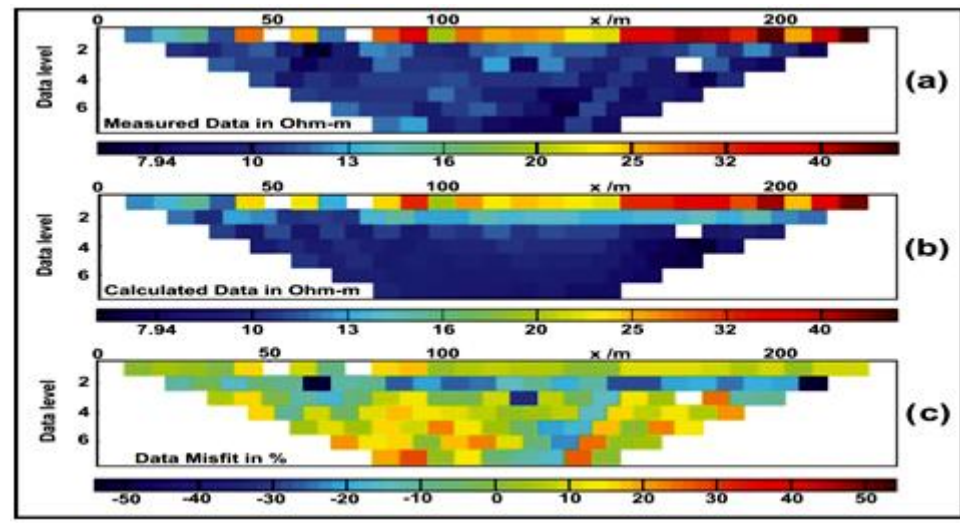


Figure (6): Calibration between the borehole information and interpretation results of sounding no.4 (for location, c.f. Figure3) using IPI2WIN program.

The 2D resistivity data were acquired and inverted to: (i) construct a 2D image of the obtained true subsurface resistivity distributions along the measured profiles, (ii) delineate the possible infiltration zones of groundwater from the rainfalls and flash floods and surface open drains and (iii) confirm the 1D inversion results. The DCR data of the 2D profile (p1) were processed and inverted using DC2DInvRes program [21] program is based on numerical modeling techniques using finite-difference (FD) method (Figure7).

In DC2DInvRes program the inversion process was carried out using high values for initial damping factor (about 0.3), in case of increased number of noisy data which reduced after each iteration. Instead of automatically decreasing the damping factor after each iteration, the “optimize damping factor” option allows the program to look for an optimum damping factor. Since the model resolution decreases with depth, the program increases the damping factor value by about 5% for each deeper layer.



Figure(7): Pseudosections of (a) the measured apparent resistivity, (b) calculated resistivity and (c) relative difference between measured and calculated resistivity of Wenner beta profile (P1), white rectangles represents rejected bad points.

5. RESULTS AND DISCUSSION

Because the rock electrical resistivity values depend mainly on clay contents, lithology, water and salinity [22], the inversion results of DCR soundings were calibrated with available borehole, surface geological and hydrogeological data. For example, the interpretation of DCR soundings and their correlation with the borehole data are shown in Figure (6). Regarding to such correlation, Figure (8) shows a resistivity spectrum for the subsurface layer distributions in the study area.

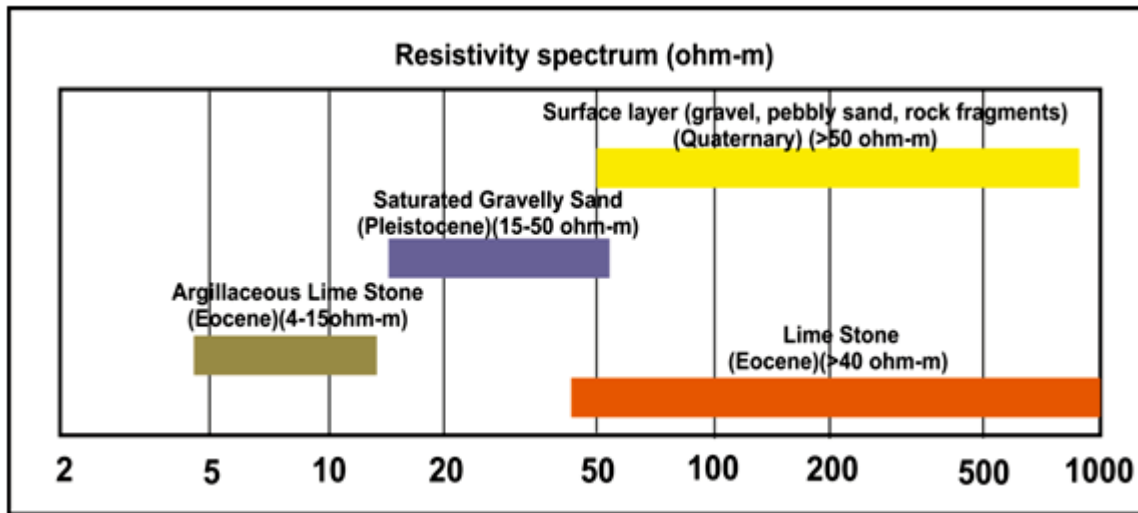


Figure (8): A resistivity spectrum showing the true resistivities based on the calibration between the inversions results of DCR soundings and available borehole data.

Based on aforementioned calibration and established resistivity spectrum, the investigated area can be divided into four geoelectrical layers. The following is brief description of the obtained calibration:

- 1- The first geoelectrical layer has specific resistivity values ranging from 50 to 1000 ohm-m which is attributed to the near surface layer consisting of Quaternary deposits (dry gravel, peppy sand with rock fragments).
- 2- The second geoelectrical layer resistivities range from 15 to 50 ohm-m. This layer is related to Pleistocene aquifer (i.e., saturated gravelly sand). The variation in resistivity values can be attributed to the degree of saturation and clay content.
- 3- The third geoelectrical layer has low to medium resistivity values (4 to 15 ohm-m). It is recognized as argillaceous limestone of Eocene age.
- 4- The fourth geoelectrical layer has resistivity values more than 40 ohm-m which corresponds to limestone with shale intercalations (Eocene).

The interpretation of DCR soundings has been inspected to recognize the number of geoelectrical layers and their depth, thickness and resistivities. This can assist to obtain the vertical and lateral variations of the main geological units. Along the wadi course (main channel), two geoelectrical cross-sections were constructed, Figure (9). The cross-sections are named (a) and (b), which are useful in defining the subsurface layer distributions. Such sections run from the northwestern to the southeastern parts (NW-SE). Figure (9) represents the constructed stitched resistivity sections along the wadi course. The inversion results of DCR soundings were interpreted to illustrate the lateral and vertical variations of electrical properties, as well as to show the hydrogeological and geological conditions in comparison with available geological and borehole data.

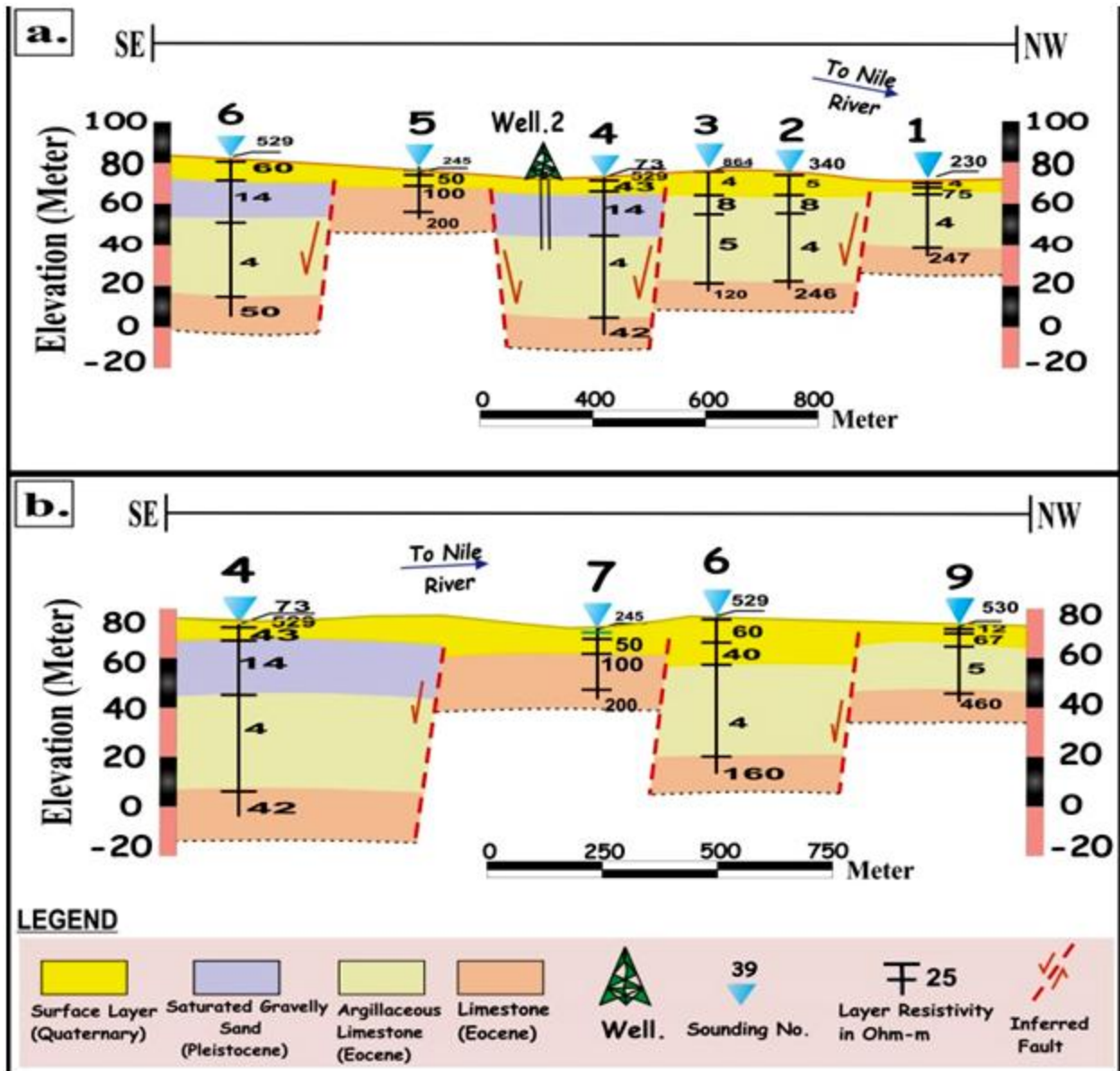


Figure (9) (a and b) Stitched resistivity sections a cross the main channel of wadi Ramleiya (For location, c.f. Figure 3).

The cross-resistivity section “a”(Figure 9) includes 6 DCR soundings (i.e. no. 1-6, for location, c.f., Figure 6). This section is ~ 2km long. The first geoelectrical layer (yellow color) corresponding to surface cover is represented by high to medium resistivity values (50-100ohm-m) with average thickness of 20m. In general, the wide range of resistivity values indicate the near surface heterogeneities along the main wadi channel, which can be attributed to gravel, pebbly sand and rock fragments. The second geoelectrical layer is represented by low resistivity values (< 10 ohm-m) corresponding to argillaceous limestone (light brown). It can be observed that the depth of second geoelectrical layer ranges from 40m (sounding No.2) to 25m (sounding No.1). It can be observed that the second geoelectrical layer overlies a high resistivity layer (> 50 m) corresponding to Eocene limestone with shale intercalations (brown color).

The cross-section a shows a shallow medium resistivity layer (16-28 ohm-m) at soundings No. 4 and 6. Regarding to geological and hydrogeological data, such layer can be corresponding to saturated gravelly sand (blue color). It can be also observed that the depth of such aquifer becomes shallower towards southeastern part (i.e. towards the downstream portions) than northwestern part (i.e. towards high plateau). Further, the thickness of the shallow aquifer ranges from 22 (sounding No.4) to 15m (sounding No, 6).

Regarding to field observations and structural geological map [14], the geoelectrical layer displacement along the constructed geoelectrical cross-section can be attributed to a fault existence. Because the actual fault locations/dips are

unknown, the inferred faults were plotted in the form of dashed lines. It can be noticed that the aquifer existence is controlled by such faults, where the uplift of Eocene rocks at soundings No. 3 and 5 forming a grabben-like structure at the central part of geoelectrical cross-section (a). Accordingly, considerable thicknesses of Pleistocene gravelly sand were deposited forming a shallow aquifer at the central part of the wadi course.

The geoelectrical cross-section “b” (Figure9) passes through four sounding points (no. 4 and 7-9, for location, c.f., Figure3). Structurally, this wadi portion is characterized by complex structures in the form of faults. Similar to the geoelectrical cross-section “a”, the cross-section “b” (~ 2 km long) represents three main geoelectrical layers (i.e. surface layer, argillaceous limestone and limestone with shale intercalations). The abovementioned shallow medium resistivity layer corresponding to Pliocene-Pleistocene aquifer can be observed at soundings No. 4 and 6 with 15 m average thickness and depth. In general, the abrupt change in the thickness and values of resistivity of geoelectrical layers can be explained by expected faults between them. Obviously, the complex inferred faults in the wadi prevent the water migration from saturated zone.

The constructed fence diagram (Figure10) shows that towards the northeastern parts of the area (i.e., G. Tarbul) the high resistivity layer corresponding to Eocene limestone rocks (orange color) are dominant. On the other hand, the low to medium resistivity layers are dominate at the western and southwestern parts corresponding to Eocene argillaceous limestone (pink color) and Pliocene-Pleistocene (light green to blue colors) deposits, respectively.

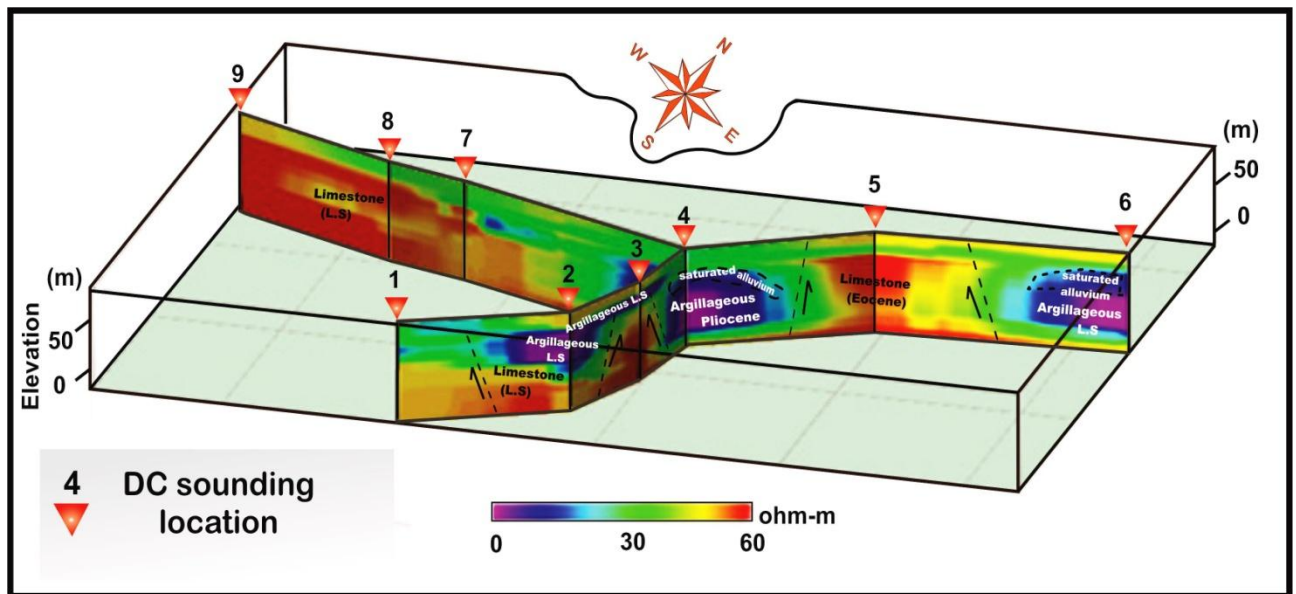


Figure (10): 3D fence diagram showing the inversion results of DCR soundings measured around downstream portion of wadi Ramleiya, for location, c.f., Figure3).

Although the DCR soundings give helpful information about the subsurface geological conditions, the results can only applied to the close vicinity of sounding points. The 2D resistivity profiling was applied to construct a 2D image confirming the presence of electrical features seen in 1D cross-sections, a and b (Figure 9). Figure (3) shows the 2D DCR profile (P1) location. It can be observed that the 2D profile was measured on the wadi downstream to record the lateral variation of subsurface structure regarding to the DCR sounding results.

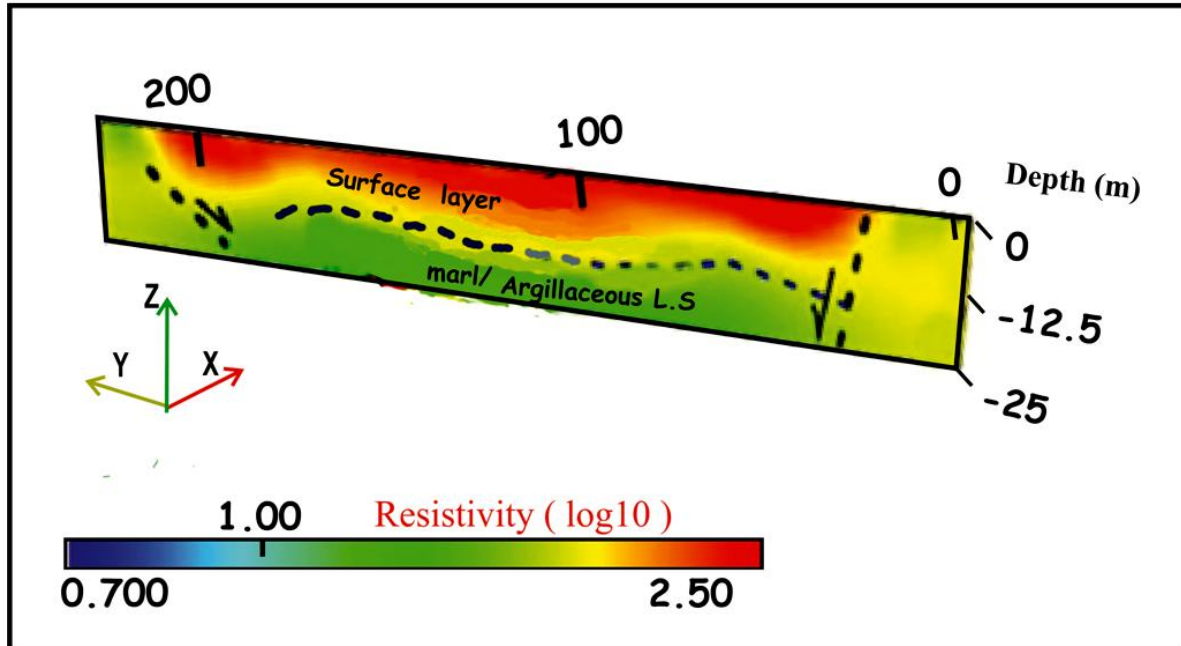


Figure (11): 2D profiles modeling (P1) measured at downstream portion of wadi Ramleiya, for location c.f., Figure3).

For 2D DCR model, the maximum depth was chosen based on the sensitivity analysis and the median depth of investigation [23] of Wenner beta array. The 2D profile (P1) provides additional information on shallow subsurface structures (Figure 11). The inverted 2D model of P1 profile shows two main geoelectrical layers. The first geoelectrical layer represents a lateral change of resistivity values, which corresponds to Pleistocene gravelly sand along the wadi. The first geoelectrical layer thickness is ~ 8 m. This layer rests on a medium resistivity layer of 50-100ohm-m corresponding to argillaceous limestone/marl layer. It can be also observed that there are lateral discontinuities along the 2D inverted model with lateral displacement. Considering the geological and structural mapping of the area, two normal faults were projected on the 2D inverted model. Notably, the wadi downstream is located between such normal faults. Accordingly, the wadi is bounded on the both sides by medium resistivity layer corresponding to impermeable argillaceous limestone/marl layer. It can be noticed that the geoelectrical layer boundaries (Figure11), especially for conductivity layer (i.e. <20 ohm-m), are distorted and layer thicknesses cannot be resolved using derivative based inversion method (DBI). These limitations were discussed in detail by [18, 24, 25]. To enhance such observed limitations in 2D-ERT using DBI method, the 2D profiles were calibrated with available boreholes and local geology of the study area.

6. CONCLUSIONS

A combination of geomorphological, geological and geophysical techniques has been applied to characterize the regional hydrogeological and structure settings at the downstream part of wadi Ramleiya, Eastern Desert, Egypt. This study provides the basis for preliminary hydrogeological assessment of wadi system. The paper indicates that the aquifers existence in the wadi is controlled by subsurface structures, i.e. faults. Geomorphological and structural evidences provide an understanding of regional geological and hydrogeological settings of the area. Then, subsurface geological and hydrogeological information is acquired by DC resistivity inversion results. The combined approach, where DC resistivity results are calibrated with borehole, geological mapping and geomorphological data, proved crucial in hydrogeophysical assessment in wadi system. The present integrative approach described through this case study will be of interest to flash hazard management in wadi system in similar geological settings.

7. REFERENCES

- [1] Attwa, M. and Henaish, A., 2018. Regional structural mapping using a combined geological and geophysical approach—A preliminary study at Cairo-Suez district, Egypt. African Earth Sciences, 144, 104-121.

- [2] Goebela, M., Pidlisecky, A. and Knight, R., 2017. Resistivity imaging reveals complex pattern of saltwater intrusion along Monterey coast. *Journal of Hydrology*, 551, 746-755.
- [3] Lysdahl A K, Bazin S, Christensen C, Ahrens S, Günther T. and Pfaffhuber A.A. 2017. Comparison between 2D and 3D ERT inversion for engineering site investigations-a case study from Oslo Harbour. *Near Surface Geophysics*, 15, 201-209.
- [4] Maurya, P.K., Rønde, V., Fiandaca, G., Balbarini, N., Auken, E., Bjerg, P.L. and Christiansen, A.V., 2017. Detailed landfill leachate plume mapping using 2D and 3D Electrical Resistivity Tomography - with correlation to ionic strength measured in screens. *Journal of Applied Geophysics*, 138, 1-8.
- [5] Attwa, M. and Günther, T., 2013. Spectral induced polarization measurements for predicting the hydraulic conductivity in sandy aquifers. *Hydrol. Earth Syst. Sci.* 17: 4079-4094.
- [6] Attwa M, Gemail K S, Eleraki M (2016) Use of salinity and resistivity measurements to study the coastal aquifer salinization in a semi-arid region: a case study in northeast Nile Delta, Egypt. *Environmental Earth Sciences*, 75: 784. <https://doi.org/10.1007/s12665-016-5585-6>
- [7] Attwa, M., Günther, T., Grinat, T. and Binot, F., 2009. Transmissivity estimation from sounding data of holocene tidal deposits in the North Eastern Part of Cuxhaven, Germany. Extended abstract: Near Surface 2009 - 15th European Meeting of Environmental and Engineering Geophysics, Dublin, Ireland, ID 6710.
- [8] Attwa, M. and Günther, T. (2012) Application of spectral induced polarization (SIP) imaging for characterizing the near-surface geology: an environmental case study at Schillerslage, Germany, *Australian Journal of Applied Sciences*, 6, 693–701, 2012.
- [9] Gemail, K.S., Attwa, M., Eleraki, M. and Zamzam, S., 2017. Imaging of wastewater percolation in heterogeneous soil using electrical resistivity tomography (ERT): a case study at east of Tenth of Ramadan City, Egypt. *Environmental earth Sciences*, 76, 666, <https://doi.org/10.1007/s12665-017-7013-y>.
- [10] Khakhar, M., Ruparelia, J.P. and Vyas, A., 2017. Assessing groundwater vulnerability using GIS-based DRASTIC model for Ahmedabad district, India. *Environmental earth Sciences*, 76: 440. <https://doi.org/10.1007/s12665-017-6761-z>.
- [11] Khan, S. and Javed, K., 2017. Geomorphometric Characteristics and Associated Land Use/Land Cover in Sajnam Basin: A Remote Sensing and GIS Based Approach. *Journal of Remote Sensing and GIS*, 8(3), 22-32.
- [12] Radwan, F., Alazba, A. and Mossad, A., 2017. Watershed morphometric analysis of Wadi Baish Dam catchment area using integrated GIS-based approach. *Arab J Geosci.*, 10: 256. <https://doi.org/10.1007/s12517-017-3046-5>.
- [13] Said, R., 1962. *The geology of Egypt*. Elsevier, Amsterdam and New York.
- [14] Conco, C., 1987. *Geological map of Egypt*, scale 1: 500,000. Geological Survey and Egyptian General Petroleum Corporation, Cairo.
- [15] Parkhomenko, E.I., 1967. Chapter 111, *Electrical Resistivity of Rocks, Electrical Properties of Rocks*, Translated from Russian and Edited by GV Keller.
- [16] Attwa, M., Akça, I., Basokur, A., Günther, T., 2014a. Structure-based geoelectrical models derived from genetic algorithms: A case study for hydrogeological investigations along Elbe River coastal area, Germany. *Journal of Applied Geophysics*, 103, 57-70.
- [17] Attwa, M. and Ali, H., 2018. Resistivity Characterization of Aquifer in Coastal Semiarid Areas: An Approach for Hydrogeological Evaluation. In: *The Handbook of Environmental Chemistry*. Springer, Berlin, Heidelberg, doi: https://doi.org/10.1007/698_2017_210.
- [18] Attwa, M., Basokur, A.T. and Akca, I., 2014b. Hydraulic conductivity estimation using direct current (DC) sounding data: A case study in East Nile Delta, Egypt. *Hydrogeology Journal*, 22, 163–1178.
- [19] Mundry, E. and Dennert, U., 1980. Das Umkehrproblem in der geophysik. *Geologisches Jahrbuch, Reihe (19)*, 19-39.
- [20] Bobachov, C., 2002. IPI2Win: windows software for an automatic interpretation of resistivity sounding data. Ph.D. thesis, Moscow state University.
- [21] Günther, T., 2004. Inversion methods and resolution analysis for the 2D/3D reconstruction of resistivity structures from DC measurements. Ph.D. thesis, Technische Univ., Freiberg, Germany.
- [22] Choudhury, K., Saha, D.K. and Chakraborty, P., 2001. Geophysical study for saline water intrusion in a coastal alluvial terrain. *Journal of Applied Geophysics*, 46, 189-200.

- [23] Edwards, L.S., 1977. A modified Pseudosection for resistivity and IP. *Geophysics*, 42, 1020-1036.
- [24] Attwa, M. , Günther, T., Grinat, T. and Binot, F., 2011. Evaluation of DC, FDEM and IP resistivity methods for imaging perched saltwater and shallow channel within coastal tidal sediments. *Journal of Applied Geophysics*, 75(4), 616-670.
- [25] Attwa, M. , and Günther, T., 2012. Application of spectral induced polarization (SIP) imaging for characterizing the near surface geology: an environmental case study at Schillersalge, Germany. *Australian journal of Applied Sciences*, 6(9), 693-701